Journal of
Materials Chemistry C

Accepted Manuscript

Graphical Abstract

Bipolar host material for PhOLEDs

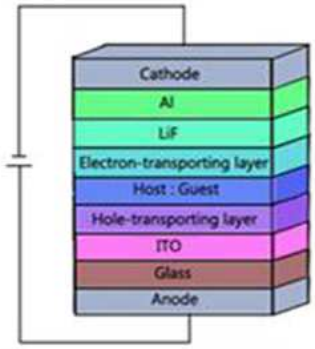

Highlights

PhOLEDs fabricated from a new bipolar host material with high triplet energy exhibit reasonable good performance

A star-shape bipolar host material based on carbazole and dimesitylboron moieties for fabrication of highly efficient red, green and blue electrophosphoresent devices

Heping Shi,*[a] Dehua Xin,[a] Xiuqing Dong,[a] Jian-xin Dai,[a] Xiaohuan Wu,[a] Yanqin Miao,[b] Li Fang,[a] Hua Wang*[b] and Martin M. F. Choi*[c]

Abstract

A new bipolar host material based on carbazole and dimesitylboron moieties, 3,6-bis(dimesitylboryl)-9-(4-(dimesitylboryl)phenyl) carbazole (**BDDPC**), has been successfully synthesised and characterised by elemental analysis, nuclear magnetic resonance spectroscopy, mass spectrometry and thermogravimetric analysis. The electrochemical and photophysical properties of **BDDPC** are studied by both experimental and theoretical methods. **BDDPC** exhibits excellent thermal stability (T_d = 234 ^oC), electrochemical stability, high fluorescence quantum yield (0.95) and high triplet energy (2.83 eV). A red phosphorescent organic light-emitting diodes (PhOLEDs) device comprising **BDDPC** as the host material and $Os(bpftz)_2(PPh_2Me)_2$ as the dopant is fabricated which displays promising electrophosphoresence properties with a turn-on voltage of 3.0 V, a maximum brightness of 12,337 cd/m^2 and a maximum current efficiency of 11.04 cd/A. Similarly, **BDDPC** is used to fabricate a green PhOLEDs device with $Ir(ppy)_2(acac)$ as the dopant, possessing a turn-on voltage of 2.5 V, a maximum brightness of 26,473 cd/m^2 and a maximum current efficiency of 38.60 cd/A. Furthermore, a blue PhOLEDs device with **BDDPC** as the host material and FIrpic as the dopant was fabricated with a turn-on voltage of 3.0 V, a maximum brightness of 7622 cd/m^2 and a maximum current efficiency of 7.39 cd/A. It is anticipated that **BDDPC** has great potential in manufacturing PhOLEDs devices for displaying or lighting applications.

***Keywords*:** Carbazole, Dimesitylboron, Photophysical properties, Host material, Electrophosphoresence

[a]*School of Chemistry and Chemical Engineering, Shanxi University, 92 Wucheng Road, Taiyuan 030006, Shanxi Province, China. E-mail:* hepingshi@sxu.edu.cn*; Fax: +86-351-7011688; Tel.: +86-351-7010588*

[b]*Key Laboratory of Interface Science and Engineering in Advanced Materials, Taiyuan University of Technology, Taiyuan 030024, Shanxi Province, China. E-mail: wanghua001@tyut.edu.cn*

[c]*Department of Chemistry, Hong Kong Baptist University, 224 Waterloo Road, Kowloon Tong, Hong Kong SAR, China. E-mail: mfchoi@hkbu.edu.hk; Fax: +852-34117348; Tel.: +852-34117839*

1. Introduction

Organic light-emitting diodes (OLEDs) have attracted a great deal of scientific and commercial interests owing to their promising applications in flat-panel display and solid-state illumination source. Besides the improvement in production process and structure of OLEDs, designing and synthesizing organic electroluminescent materials with excellent performance is of great importance for their commercialization. Organic electroluminescent materials are commonly classified as organic electroluminescent fluorescent and phosphorescent materials based on their luminescent mechanisms.[1,2] The organic electroluminescent fluorescent materials emit light by using the singlet state exciton. Unfortunately, the luminescence efficiency of devices made by fluorescent materials is low in general. As such, the improvement of the luminous efficiency of device has become an essential research topic in the organic electroluminescent field.

In 1998, Forrest and his co-workers successfully prepared a luminous layer of OLED using platinum-porphyrin complexes as the phosphor object materials and tris(8-hydroxyquinoline) aluminium with electron transport properties as the host material by co-evaporation. The luminous efficiencies of their electroluminescent devices were greatly improved with the external quantum efficiency of 4 and 8%.[1] Since then, OLEDs based on phosphorescent emitters of transitional metal complexes have attracted intensive attention owing to their ability to achieve an internal quantum efficiency of 100% by harvesting both singlet and triplet excitons.[1,3] To minimize self-quenching and triplet-triplet annihilation for phosphorescent OLEDs, the emitters are normally dispersed in a host matrix as emitting guests. Thus, suitable host materials are indispensable to the high performance phosphorescent devices.[4-6]

In order to prevent reverse energy transfer from the guest back to the host and to confine the excitons on guest molecules, the excellent host materials should have higher triplet energy than that

of the guest.[7-9] Moreover, it is desirable that the host material should have good carrier transport properties for a balanced carrier recombination in the emitting layer.[10,11] So far carbazoles are considered as a prominent class of materials that can fulfil the above-mentioned requirements. Kang et al. synthesized a carbazole-type host material containing tetraphenylsilane moiety for green phosphorescent OLEDs. They found that $Ir(ppy)_3$-based OLEDs using the carbazole-type host material exhibited the maximum external quantum efficiency of 19.8%, the power efficiency of 59.4 lm/W and an initial luminance of 100 cd/m^2.[12] Very recently, Pu et al. synthesized two new carbazole-based host materials, 1,3-bis(3-(3,6-di-*n*-butylcarbazol-9-yl)phenyl)benzene (BCzPPh) and 4,6-bis(3-(3,6-di-*n*-butylcarbazol-9-yl)phenyl)pyrimidine. They observed that BCzPPh host doped with a green phosphorescent emitter displayed power efficiencies and external quantum efficiencies above 30 lm/W and 13%, respectively.[13] In principle, a favourable host material should give rise to a balanced carrier recombination in the emitting layer; thus, they ought to exhibit equal hole and electron mobility. Generally, the hole mobility of many hosts is much higher than the electron mobility since they mainly consist of strong electron donors such as carbazoles and aromatic amines.[14] An effective approach to optimize the hole and electron mobilities is to use bipolar host materials. Wong and co-workers developed a series of novel bipolar host materials incorporating the electron-donating carbazole core and electron-accepting moieties such as benzimidazole, phenylbenzimidazole, 1,3,5-triazine diarylborane, which generally exhibited high morphological and thermal stability, suitable energy levels, and balanced electron/hole transporting characteristics. Devices based on those materials demonstrated better external quantum efficiencies, indicating the great potential of bipolar materials in OLEDs.[15-19] Moreover, Zhuang et al. developed a series of bipolar host materials containing carbazole and 1,2,4-triazole building blocks. Devices based on the bipolar host materials exhibit better performance than those based on

4,4'-*N*,*N*'-dicarbazole-biphenyl and 1,3-bis(9-carbazolyl)benzene. The best host material could achieve efficiencies at 32.7 and 21.1 cd/A for green and blue devices, respectively.[20] Recently, Huang et al. synthesized a series of bipolar hosts based on benzimidazole-carbazole cores and fabricated highly efficient blue and single-emitting layer white devices using the bipolar compounds as host materials. The devices hosted by 9-(3-(1-Phenyl-1H-benzo[d]imidazol-2-yl)phenyl)-9H-carbazole (**mBICP**), 5-(3-(1-Phenyl-1H-benzo[d]imidazol-2-yl)phenyl)-5H-pyrido[4,3-b]indole (**mBINCP**) and 9-Phenyl-3-(3-(1-phenyl-1H-benzo[d]imidazol-2-yl)phenyl)-9H-carbazole (**mBIPhCP**) obtain maximum external quantum efficiencies of 18.7, 13.8 and 17.0% for blue phosphorescent organic light-emitting diodes (PhOLEDs), respectively. The white devices hosted by mBICP, mBINCP and mBIPhCP acquire a maximum external quantum efficiency of 20.5, 12.7 and 16.6%, corresponding to a maximum power efficiency of 53.3, 31.7 and 39.4 lm W^{-1}, respectively.[21] Besides, some other groups have also done impressive work on the exploration of bipolar host materials based on carbazole.[22-26]

Triarylboron compounds have attracted a considerable attention attributing to their intriguing electronic and photophysical properties.[27,28] These excellent properties derived from the p-π conjugation between the vacant p-orbital on the boron centre and the π-orbital of the π-conjugated molecular system.[29-33] Recently, many triarylboron compounds have been synthesized as nonlinear optical materials, charge-transport and emissive materials in OLEDs.[34-41] As such, triarylboron compounds possessing high effective photoelectric and transmission performance should be ideal materials for organic electroluminescent devices. Lin et al. synthesized a new bipolar host material (CMesB) containing the dimesityl borane/carbazole hybrid. They reported that red/green/blue/white OLEDs based on CMesB all show high external quantum efficiencies. The results indicated that

CMesB is a promising universal host material for phosphorescent OLEDs of various colours.[42]

In this work, we propose to combine triarylboron compounds and carbazoles into a single molecular unit in order to further improve the luminescent, hole-transporting and electron-transporting performance of PhOLEDs device. A novel star-shape compound based on carbazole and dimesitylboron moieties, 3, 6-bis(dimesitylboryl)-9-(4'-(dimesitylboryl)phenyl)carbazole (**BDDPC**), was synthesized by introducing triarylboron units to the 3,6-positions and 9-(4-phenyl) position of a carbazole. The chemical structure of **BDDPC** was fully characterized by proton nuclear magnetic resonance (^{1}H NMR), ^{13}carbon (^{13}C NMR) spectroscopy, mass spectrometry (MS) and elemental analysis. The thermal, electrochemical, photoluminescent and electrophosphoresent properties of **BDDPC** were studied in detail. Finally, **BDDPC** was employed as a host material for fabricating a red, a green and a blue PhOLEDs device with excellent electroluminescent properties. It is anticipated that **BDDPC** will be a new and promising host material in phosphorescent organic electroluminescent devices for displaying or lighting applications

2.1. Experimental

2.1. Synthesis of 9-(4'-bromophenyl)carbazole (1)

The synthesis routes are summarized in Scheme 1. A mixture of carbazole (5.02 g, 30 mmol), 1-bromo-4-iodobenzene (8.49 g, 30 mmol), 18-crown-6 (0.40 g, 1.5 mmol), K_2CO_3 (8.29 g, 60 mmol) and CuI (0.57 g, 3.0 mmol) and 1,3-dimethyl-3,4,5,6-tetrahydro-2(1H)-pyrimidinone (10 mL) was heated at 170 °C under nitrogen (N_2) for 18 h. After cooling to room temperature, the reaction was quenched with ice water. The mixture was extracted with CH_2Cl_2, washed with water, and dried over Na_2SO_4. After the solvent had been completely removed, the residue was purified by

column chromatography on silica gel (CH_2Cl_2/hexane) to afford the desired product as a white solid (**1**) (7.65 g, 79% yield). ^{1}H NMR (600 MHz, $CDCl_3$) δ 8.13 (dd, *J* = 7.8, 0.5 Hz, 2H), 7.92 (d, *J* = 8.3 Hz, 2H), 7.39 (m, 4H), 7.32 (d, *J* = 8.3 Hz, 2H), and 7.29 (t, *J* = 7.3 Hz, 2H).

Scheme 1

2.2. Synthesis of 3,6-dibromo-9-(4'-bromophenyl)carbazole (2)

N-Bromosuccinimide (2.0 g NBS, 11.0 mmol) in dimethylformamide (10 mL DMF) was added dropwise to a solution of **1** (1.6 g, 5.0 mmol) in DMF (20 mL) at 0 °C. The mixture was stirred for 3 h at room temperature. Then, ice water was added to the mixture to give a white precipitate. The obtained white solid was purified by flash silica-gel column chromatography using petroleum ether as eluent to afford 3,6-dibromo-9-(4'-bromophenyl)carbazole (**2**). ^{1}H NMR (600 MHz, $CDCl_3$) δ 8.19 (d, *J* = 2.0 Hz, 2H), 7.74 (d, *J* = 8.7 Hz, 2H), 7.51 (dd, *J* = 8.7, 1.7 Hz, 2H), 7.38 (d, *J* = 8.7 Hz, 2H), and 7.22 (d, *J* = 8.7 Hz, 2H).

2.3. Synthesis of 3, 6-bis(dimesitylboryl)-9-(4'-(dimesitylboryl)phenyl)carbazole (BDDPC)

To a solution of **2** (0.48 g, 1.0 mmol) in anhydrous tetrahydrofuran (40 mL THF), *tert*-butyllithium (1.6 M *t*-BuLi solution) in *n*-hexane (3.75 mL, 6.0 mmol) was injected at -78 °C under N_2. The reaction was kept at this temperature for 3 h, and dimesitylboron fluoride (1.69 g Mes_2BF, 6.3 mmol) in THF (20 mL) was added dropwise. The temperature was allowed to rise to room temperature and the mixture was stirred overnight. Then, water was added and the mixture was extracted with CH_2Cl_2, washed with water, dried over Na_2SO_4. After the solvent had been completely removed, the residue was purified by column chromatography (CH_2Cl_2/*n*-hexane) to obtain **BDDPC**. ^{1}H NMR (600 MHz, $CDCl_3$) δ 8.35 (s, 2H), 7.74 (d, *J* = 8.1 Hz, 3H), 7.57 (m, 4H), 7.38 (d, *J* = 8.3 Hz, 2H), 6.85 (s, 4H), 6.82 (s, 8H), 2.26 (s, 6H), 2.25 (s, 12H), 2.02 (s, 12H), 2.01

(s, 24H). ^{13}C NMR ($CDCl_3$): d 142.8, 139.7, 134.2, 133.7, 132.6, 132.3, 132.2, 132.0, 131.2, 130.3, 128.8, 128.5, 126.8, 125.7, 125.3, 123.9, 123.3, and 110.2. Anal. calcd for $C_{54}H_{40}NO_3B_3$: C, 76.86; H, 4.78; N, 1.66. Found: C, 75.90; H, 4.77; N, 1.58. LC-MS (*m*/*z*): 844.2 $[M + H]^+$.

2.4. Measurement and characterization

Melting points were determined on an X-5 melting point detector. All NMR spectra were measured on a Bruker 600 MHz spectrometer. Thermogravimetric analysis (TGA) was performed on a TGA 2050 thermogravimetric analyser under N_2 atmosphere with a heating rate of 10 °C/ min from room temperature to 750 °C. Elemental analyses were performed on an Element Analysis System. Mass spectra were recorded with a LC-MS system consisted of a Waters 1525 pump and a Micromass ZQ4000 single quadrupole mass spectrometer detector. Cyclic voltammetry (CV) was performed on a CHI-600C electrochemical analyser. The CV measurements were carried out with a conventional three-electrode configuration consisting of a glassy carbon working electrode, a platinum-disk auxiliary electrode and a Ag/AgCl reference electrode, and the scan speed was 50 mV/s. UV-vis absorption spectrum was acquired on a Shimadzu UV-2450 spectrophotometer. Fluorescence spectra were obtained on a Hitachi F-4500 spectrofluorometer. Fluorescence quantum yield was determined by using quinine sulfate as the reference. All measurements were performed at room temperature.

2.5. Device fabrication and testing

The multilayer OLEDs were fabricated by the vacuum-deposition method. Organic layers were deposited by high-vacuum (5×10^{-4} Pa) thermal evaporation onto a glass (3 cm×4 cm) substrate pre-coated with an indium tin oxide (ITO) layer. *N*,*N*-bis(naphthyl)-*N*,*N*-bis(phenyl)benzidine,

4,4'-bis(*N*-carbazolyl)-1,1'-biphenyl, **BDDPC**, 4,7-diphenyl-1,10-phenanthroline (BPhen), and LiF/Al were used as the hole-transport layer, electron-blocking layer, emitting layer, electron-transport layer and cathode, respectively. All organic layers were sequentially deposited. Thermal deposition rates for organic materials, LiF and Al were 0.5, 0.5 and 1 Å/s, respectively. The active area of the devices was 12 mm^2. The electroluminescent spectra were measured on a Hitachi MPF-4 spectrofluorometer. The voltage–current density (V–J) characteristics of OLEDs were recorded on a Keithley 2400 Source Meter. The characterization of brightness–current–voltage (B–I–V) were measured with a 3645 DC power supply combined with a 1980A spot photometer and were recorded simultaneously. All measurements were done at room temperature in ambient conditions.

2.6. Theoretical calculations

The ground-state geometry of **BDDPC** was optimized at B3LYP level with 6-31G (d, p) basis set.[43-45] The vibration frequencies and the frontier molecular orbital characteristics were analysed on the optimal structure at the same level. The excited-state geometry of compound was optimised based on the ground state structures using time-dependent density functional theory (DT-DFT) method at B3LYP level with 6-31G (d, p) basis set. The absorption and emission spectra of compound were carried out using TD-DFT method based on the optimal ground state structure and the lowest singlet excited state structure, respectively. Solvent effect was also taken into account by using the polarised continuum model.[46,47] All calculations were carried out with the Gaussian 09 program package[48] and performed in the Supercomputing Centre of Computer Network Information Centre of the Chinese Academy of Sciences.

3. Results and discussion

3.1. Synthesis and characterization

Scheme 1 displays the synthetic route of **BDDPC**. First, Compound **1** was synthesized via the modified Ullmann reaction. Then, Compound **2** was prepared by bromination of **1** with NBS. The final product **BDDPC** was obtained by reacting **2** with *t*-BuLi, followed with the addition of Mes_2BF. The chemical structure of **BDDPC** was fully characterized by ^1H NMR, ^{13}C NMR and MS. The ^1H NMR spectrum of **BDDPC** displays downfield peaks at 7.00–8.48 ppm which were assigned to the protons of carbazole moieties. The downfield peaks at 6.59–6.89 ppm and the upfield peaks at 2.09 and 2.37 ppm were corresponding to the dimesitylboron moieties protons. The ^{13}C NMR, MS and elemental analysis are consistent with the desirable structures. Our synthesis routes successfully synthesized **BDDPC** which is soluble in many common organic solvents including CH_2Cl_2, $CHCl_3$, DMF, THF, toluene, and dimethylsulfoxide.

3.2. Thermal properties

The thermal property of **BDDPC** was investigated by TGA and differential scanning calorimetry (DSC) under N_2 atmosphere as depicted in Fig. S1 and Fig. S2 (ESI), respectively. The decomposition temperature (T_d) corresponding to 5% weight loss of **BDDPC** is at 234 °C and a glass transition temperature (T_g) is at 110 °C. These results are summarized in Table 1. The high T_d might be attributed to its large molecular mass, the rigid carbazole core and the non-planar dimesitylboron peripheries. The result indicates that **BDDPC** has good thermal stability and high T_g which should be adequate for most optoelectronic device applications.

3.3. Theoretical calculation

Theoretical calculations can provide a reasonable qualitative indication of the excitation and

emission properties of a compound.[49] **BDDPC** comprise a 9-phenylcarbazole unit as the core and three dimesitylboron units as the terminals. Its geometry at ground state was optimised at the DFT/B3LYP/6-31G (d, p) level by using Gaussian 09 software. Fig. 1 depicts the carbazole moiety is of planar structure and the three mesityl groups form propeller-like conformations originated from the trigonal boron centre. The highest occupied molecular orbital (HOMO) and the lowest unoccupied molecular orbital (LUMO) of **BDDPC** (Fig. 1) were also calculated at DFT/B3LYP/6-31G (d, p) level using the polarised continuum model for geometry optimisations. The HOMO is localized mainly in the carbazole moiety while the LUMO is in the dimesitylborylphenyl moiety. Thus, the electronic transition from the ground state to the first excited state mainly involves intramolecular charge transfer (ICT) from the carbazole (electron-donor) to the dimesitylborylphenyl (electron-acceptor) moieties.

Generally, holes and electrons in OLEDs are transferred through the individual HOMO and LUMO levels.[50] **BDDPC** exhibits complete separation and localisation of HOMO and LUMO, inferring that the HOMO to LUMO transition follows a typical charge transfer process. In addition, the complete localisation of HOMO and LUMO is essential to the efficient hole and electron transport and to the prevention of reverse energy transfer as well.[51] Table 1 displays the calculated HOMO and LUMO energy levels of **BDDPC** at -5.55 and -1.90 eV, respectively. The HOMO-LUMO energy gap (E_g) is 3.65 eV. The theoretical E_g is *ca.* 0.39 eV larger than the optical energy band gap obtained from UV-vis absorption measurement.

Fig. 1

Table 1

3.4. Photophysical properties

Fig. 2 displays the UV-vis absorption, fluorescence and phosphorescence emission spectra of **BDDPC** in THF (10 μM). The spectroscopic data are summarized in Table 1. **BDDPC** exhibits two major absorption bands at 290–330 and 330–380 nm. The absorption peak maximum (λ_{abs}) at 348 nm is corresponding to the π-π* electronic transition and the λ_{abs} of 390 nm is assigned to the ICT

from the carbazole core to dimesitylboron terminal. The optical energy band gap calculated from the absorption band edge of the absorption spectrum is approximately 3.26 eV. **BDDPC** exhibits a strong fluorescence emission band at 369–550 nm with an emission peak maximum (λ_{em}) of 420 nm. The emission band is assigned to ICT from the carbazole core to dimesitylboron terminal. The fluorescent quantum yield (Φ) of BDDICZ in THF solvent was measured by using quinine sulfate in 0.10 M sulfuric acid as the reference.[52] **BDDPC** possesses a high Φ of 0.95, revealing its potential application as an excellent optoelectronic material in optical field.

The phosphorescence emission spectrum of **BDDPC** was performed in a frozen THF at 77 K in order to determine its triplet energy (E_T). The highest-energy phosphorescence peak is 438 nm and the triplet energy is 2.83 eV. Such the triplet energy implies that **BDDPC** could serve as an appropriate host material for red and green phosphors. This result clearly suggests the effective interruption of π-conjugation between carbazole core and three dimesitylboron terminals due to the highly twisted conformation.

Fig. 2

3.5. Electrochemical properties

The electrochemical properties of **BDDPC** were studied by CV with Ag/AgCl as the reference electrode. The measurement was conducted in 1.0 mM **BDDPC** in acetonitrile containing 0.10 M tetrabutylammonium perchlorate as the supporting electrolyte under N_2 atmosphere. The CV of **BDDPC** is displayed in Fig. S3 (ESI). A reversible oxidation peak and three reversible reduction peaks are observed within the entire electrochemical window of acetonitrile. The reversible oxidation peak around +1.34 V is assigned to the oxidation of carbazole, whereas three reversible reduction peaks around -0.99, -2.06 and -2.28V are attributed to the electron injection into the vacant *p*-orbital of dimesitylboron.[42] Obviously, the higher reduction potentials (-0.99V) of **BDDPC** suggest the electron distributions on its LUMO are solely localised on the dimesitylborylphenyl moiety.[15] The HOMO energy level can be calculated with the empirical

equation: HOMO = – (E_{ox} + 4.40) eV, where E_{ox} is the onset oxidation potential.[53] The E_{ox} is 1.21 eV and the HOMO energy level of **BDDPC** is -5.61 eV. The E_g is estimated to be 3.26 eV by the absorption edges of the absorption spectrum. The LUMO energy level of **BDDPC** is thus -2.35 eV which is calculated from the HOMO energy level and E_g. The HOMO, LUMO and E_g are very close to the theoretical values. All the data are summarized in Table 1.

The HOMO level of **BDDPC** is well matched with those of two common hole-transporting materials, 4,4-bis[*N*-(1-naphthyl)-*N*-phenyl-aminobiphenyl (5.4 eV)[54] and 4,4′-cyclohexylidenebis[*N*,*N*-bis(4-methylphenyl)benzenamine] (TAPC) (5.5 eV),[55] indicating that **BDDPC** can possibly facilitate hole injection and transportation. Similarly, the LUMO level of **BDDPC** is also well matched with those of two common electron-transporting materials, 1,3,5-tris(1-phenyl-1H-benzimidazol-2-yl)benzene (2.39 eV) and 2,9-dimethyl-4,7-diphenyl-1,10-phenanthroline () (2.44 eV). The barrier of electron transport from the electron-transporting materials to the host materials is quite small and thus is beneficial to be used as electron-transporting materials for OLEDs.[20] The electrochemical properties of **BDDPC** indicate that it can be utilized both as a hole and an electron transporter. Furthermore, the low HOMO energy level of **BDDPC** suggests that the compound has high oxidative stability.[56] Its electrochemical stability will improve the life-time of electroluminescent devices. It is anticipated that **BDDPC** should be a desirable host material in light-emitting applications.

3.6. Charge transporting properties

Single carrier devices were fabricated to investigate the charge transporting properties of **BDDPC**. First, a hole-only device comprising ITO/TAPC (8 nm)/**BDDPC** (30 nm)/TAPC (8 nm)/Al was prepared to examine the hole transporting capability of **BDDPC**. Since TAPC has a high LUMO

level, it was used to block the electron from the cathode. Second, an electron-only device consisting of ITO/BCP (8 nm)/**BDDPC** (30 nm)/BCP (8 nm)/LiF (1 nm)/Al was prepared to examine the electron transporting capability of **BDDPC**. BCP was used to block the hole from the anode because of its low HOMO level. Fig. 3 depicts the current-characteristics of these two devices as a function of the average electric field. Both of these devices could conduct significant currents, indicating that **BDDPC** possesses the bipolar transporting property. The electron-only device conducts higher current than that of the hole-only device under the same average electric field. Although **BDDPC** has the bipolar transporting capability, its electron-transport is better than its hole-transport ability.

Fig. 3

3.7. Electroluminescent property

To evaluate **BDDPC** as the potential host material for fabrication of OLEDs, phosphorescent OLEDs were made with **BDDPC** as the host and 8.0 weight (wt) % $Ir(ppy)_2(acac)$ or $Os(bpftz)_2(PPh_2Me)_2$ as the dopant. The first device was a red phosphorescent OLED (Device R) with the configuration of ITO/TAPC (50 nm)/**BDDPC** doped with 8.0 wt % $Os(bpftz)_2(PPh_2Me)_2$ (30 nm)/tris[3-(3-pyridyl)-mesityl]borane (3TPYMB) (60 nm)/LiF (0.5 nm)/Al(150 nm). TAPC, 3TPYMB and **BDDPC** doped with 8.0 wt % $Os(bpftz)_2(PPh_2Me)_2$ were used as the hole-injection layer, electron-transporting layer and emitting layer, respectively. Fig. S4 (ESI) displays the normalized electroluminescence spectra of Device R under various applied voltages. All the spectra show the same spectral characteristics with an emission peak of 624 nm which are almost identical with the International Commission on Illumination (CIE) coordinates of (0.62,0.31), corresponding to the emission of $Os(bpftz)_2(PPh_2Me)_2$. As **BDDPC** has higher E_T than that of $Os(bpftz)_2(PPh_2Me)_2$,[57] no additional emission from the host material was observed, indicating that

Device R has very efficient energy transfer from the host to the dopant. Fig. 4 and 5 display the current density–voltage–luminance curve and current density–luminance efficiency curve of Device R, respectively. Table 2 summarizes the electroluminescent characteristics of Device R. Device R exhibits a turn-on voltage of 3.0 V and a maximum luminance efficiency (L_{max}) of 11.04 cd/A and a maximum luminance ($\eta_{L,max}$) of 12,337 cd/m^2.

Fig. 4

Fig. 5

Table 2

Similarly, a green phosphorescent OLED (Device G) with the configuration of ITO/TAPC (50 nm)/**BDDPC** doped with 8.0 wt % Ir(ppy)$_2$(acac)(25 nm)/BPhen (20 nm)/BPhen doped with 5.0 wt % of Cs_2CO_3 (30 nm)/Ag (150 nm) was prepared. TAPC, BPhen, BPhen doped with 5.0 wt % of Cs_2CO_3, and **BDDPC** doped with 8.0 wt % Ir(ppy)$_2$(acac) function as the hole-injection layer, electron-transporting layer, conductivity enhancement and electron-injection, and emitting layer of Device G, respectively. The electroluminescence spectra of Device G at various applied voltages are depicted in Fig. S5. All spectra show similar spectral characteristics with an λ_{EL} of 508 nm and almost identical with the CIE coordinates of (0.30, 0.61), corresponding to the emission of Ir(ppy)$_2$(acac). Furthermore, no additional emission coming from the host materials was observed owing to the higher E_T of **BDDPC** than that of Ir(ppy)$_2$(acac).[57] The result indicates that Device G has efficient energy transfer from the host to the dopant. Fig. 6 and 7 display the current density–voltage–luminance curves and current density–luminance efficiency curve of Device G, respectively. Table 2 summarizes the electroluminescent characteristics of Device G. Device G exhibits a turn-on voltage of 2.5 V and a L_{max} of 38.60 cd/A and a $\eta_{L,max}$ of 26,473 cd/m^2.

Fig. 6

Fig. 7

Furthermore, a blue phosphorescent OLED (Device B) with the configuration of ITO/TAPC (50 nm)/**BDDPC** doped with 15 wt % bis[2-(4,6-difluorophenyl)pyridinato-C^2,*N*](picolinato)iridium(III) (FIrpic) (25 nm)/BPhen (40 nm)/LiF (0.5 nm)/Al (150 nm) was fabricated. TAPC, BPhen, and **BDDPC** doped with 15 wt % FIrpic function as the hole-injection layer, electron-transporting layer, and emitting layer of Device B, respectively. The electroluminescence spectra of Device B at various applied voltages are depicted in Fig. S6. All spectra show similar spectral characteristics with an λ_{EL} of 472 nm and almost identical with the CIE coordinates of (0.16, 0.33), corresponding to the emission of FIrpic. Moreover, no additional emission coming from the host materials was observed owing to the higher E_T of **BDDPC** than that of FIrpic.[57] The result indicates that Device B has efficient energy transfer from the host to the dopant. Fig. 8 and 9 display the current density–voltage–luminance curves and current density–luminance efficiency curve of Device B, respectively. Table 2 summarizes the electroluminescent characteristics of Device B. Device B exhibits a turn-on voltage of 3.0 V and a L_{max} of 7.39 cd/A and a $\eta_{L,max}$ of 7622 cd/m^2.

Fig. 8

Fig. 9

The remarkable performance of Device R, G and B could be attributed to the excellent thermal stability which significantly enhances the capability of forming stable amorphous thin films. The brilliant bipolar charge transport capability of **BDDPC** significantly increases the carrier balance between the emitting layer and the high triplet energy of **BDDPC** and transfers energy from the host to the dopant. It should be pointed out that the electroluminescent performance was obtained in a non-optimized test device under ordinary laboratory conditions. The device performance could be

further improved by optimizing the layer thicknesses and processing conditions.[58] This work is currently conducted in our laboratories.

4. Conclusion

In summary, a new bipolar host material based on carbazole and dimesitylboron moieties, **BDDPC**, has been successfully synthesised and characterised by elemental analysis, NMR, MS, and TGA. The electrochemical and photophysical properties of **BDDPC** were studied by both experimental and theoretical methods. Our results demonstrate that **BDDPC** has excellent thermal stability (T_d = 234 ^oC), electrochemical stability and high Φ (0.95) as well as high triplet energy (2.83 eV). Moreover, utilizing **BDDPC** as the host material, red, green and blue PhOLEDs devices can be fabricated with relatively good brightness and current efficiency. This work demonstrates that the bipolar host **BDDPC** has potential in producing PhOLEDs devices for display or lighting applications.

Acknowledgements

This work was supported by the Natural Science Foundation of Shanxi Province (2013011013-1); Scientific and Technological Innovation Programs of Higher Education Institutions in Shanxi Province (2012005); Program for Changjiang Scholar and Innovation Research Team in University (IRT0972); International Science & Technology Cooperation Program of China (2012DFR50460); National Natural Scientific Foundation of China (21101111, 61205179, 61307030, 61307029); Shanxi Provincial Key Innovative Research Team in Science and Technology (2012041011); Shanxi Scholarship Council of China (2012-006); Hundred Talent Programme of Shanxi Province, and Fund of Key Laboratory of Optoelectronic Materials Chemistry and Physics, Chinese Academy of Sciences (2008DP173016). The authors express their sincere thanks to the Advanced Computing Facilities of the Supercomputing Centre of Computer Network Information Centre of Chinese Academy of Sciences for all the theoretical calculations.

References

1 M. A. Baldo, D. F. O'Brien, Y. You, A. Shoustikov, S. Sibley, M. E. Thompson and S. R. Forrest, *Nature*, 1998, **395**, 151-154.

2 M. A. Baldo, S. Lamansky, P. E. Burrows, M. E. Thompson and S. R. Forrest, *Appl. Phys. Lett.*, 1999, **75**, 4 (1-3).

3 M. A. Baldo and D. F. O'Brien, *Phys. Rev. B*, 1999, **60**, 14422-14428.

4 C. Adachi, M. A. Baldo, M. E. Thompson and S. R. Forrest, *J. Appl. Phys.*, 2001, **90**, 5048-5051.

5 Y. Tao, Q. Wang, C. Yang, Q. Wang, Z. Zhang, T. Zou, J. Qin and D. Ma, *Angew. Chem. Int. Ed.*, 2008, **47**, 8104-8107.

6 E. Holder, B. M. W. Langeveld and U. S. Schubert, *Adv. Mater.*, 2005, **17**, 1109-1121.

7 C. Adachi, R. C. Kwong, P. Djurovich, V. Adamovich, M. A. Baldo, M. E. Thompson and S. R. Forrest, *Appl. Phys. Lett.*, 2001, **79**, 2082 (1-3).

8 I. Avilov, P. Marsal, J. L. Bredas and D. Beljonne, *Adv. Mater.*, 2004, **16**, 1624-1629.

9 C. Ulbricht, B. Beyer, Friebe, A. Winter and U. S. Schubert, *Adv. Mater.*, 2009, **21**, 4418-4441.

10 S. Tokido, H. Tanaka, N. Noda, A. Okada and T. Taga, *Appl. Phys. Lett.*, 1997, **70**, 1929 (1-3).

11 P. Fenter, F. Schreiber, V. Buloviæ and S. R. Forrest, *Chem. Phys. Lett.*, 1997, **277**, 521-526.

12 J.-W. Kang, D.-S. Lee, H.-D. Park, J. W. Kim, W.-I. Jeong, Y.-S. Park, S.-H. Lee, K. Gob, J.-S. Lee and J.-J. Kim, *Org. Electron.*, 2008, **9**, 452-460.

13 N. Aizawa, Y.-J. Pu, H. Sasabe and J. Kido, *Org. Electron*., 2012, **13**, 2235-2242.

14 M. M. Rothmann, S. Haneder, E. Da Como, C. Lennartz, C. Schildknecht and P. Strohriegl, *Chem. Mater.*, 2010, **22**, 2403-2410.

15 Y.-M. Chen, W.-Y. Hung, H.-W. You, A. Chaskar, H.-C. Ting, H.-F. Chen, K.-T. Wong and Y.-H. Liu, *J. Mater. Chem.*, 2011, **21**, 14971-14978.

16 W.-Y. Hung, L.-C. Chi, W.-J. Chen, E. Mondal, S.-H. Chou, K.-T. Wong and Y. Chi, *J. Mater. Chem.*, 2011, **21**, 19249-19256.

17 M.-S. Lin, S.-J. Yang, H.-W. Chang, Y.-H. Huang, Y.-T. Tsai, C.-C. Wu, S.-H. Chou, E. Mondal and K.-T. Wong, *J. Mater. Chem.*, 2012, **22**, 16114-16120.

18 C.-H. Chang, M.-C. Kuo, W.-C. Lin, Y.-T. Chen, K.-T. Wong, S.-H. Chou, E. Mondal, R. C. Kwong, S. Xia, T. Nakagawa and C. Adachi., *J. Mater. Chem.*, 2012, **22**, 3832-3838.

19 H.-C. Ting, Y.-M. Chen, H.-W. You, W.-Y. Hung, S.-H. Lin, A. Chaskar, S.-H. Chou, Y. Chi, R.-H. Liu and K.-T. Wong, *J. Mater. Chem.*, 2012, **22**, 8399-8407.

20 J. Y. Zhuang, W. M. Su, W. F. Li, Y. Y. Zhou, Q. Shen and M. Zhou, *Org. Electron.*, 2012, **13**, 2210-2219.

21 H. Huang, X. Yang, B. Pan, L. Wang, J. Chen, D. Ma and C. Yang, *J. Mater. Chem.*, 2012, **22**, 13223-13230.

22 L. Zeng, T. Y.-H. Lee, P. B. Merkel and S. H. Chen, *J. Mater. Chem.*, 2009, **19**, 8772-8781.

23 J. Ding, Q. Wang, L. Zhao, D. Ma, L. Wang, X. Jing and F. Wang, *J. Mater. Chem.*, 2010, **20**, 8126-8133.

24 S. Gong, Y. Chen, X. Zhang, P. Cai, C. Zhong, D. Ma, J. Qin and C. Yang, *J. Mater. Chem.*, 2011, **21**, 11197-11204.

25 S. O. Jeon and J. Y. Lee, *J. Mater. Chem.*, 2012, **22**, 7239-7244.

26 C.-S. Wu, J.-W. Wu and Y. Chen, *J. Mater. Chem.*, 2012, **22**, 23877-23884.

27 (*a*) T. W. Hudnall, C.-W. Chiu and F. Gabbai, *Acc. Chem. Res.*, 2009, **42**, 388-397; (*b*) N. Kitamura, E. Sakuda and Y. Ando, *Chem. Lett.*, 2009, **38**, 938-943; (*c*) C. R. Wade, A. E. J. Broomsgrove, S. Aldridge and A. P. Gabba, *Chem. Rev.*, 2010, **110**, 3958-3984.

28 (*a*) A. Caruso, Jr. and J. D. Tovar, *Org. Lett.*, 2011, **13**, 3106-3109; (*b*) E. Sakuda, Y. Ando, A. Ito and N. Kitamura, *J. Phys. Chem. A*, 2010, **114**, 9144-9150.

29 (*a*) S.-C. Lo and P. L. Burn, *Chem. Rev.*, 2007, **107**, 1097-1116; (*b*) J. Li and D. Liu, *J. Mater. Chem.*, 2009, **19**, 7584-7591; (*c*) Z. M. Hudson and S. Wang, *Acc. Chem. Res.*, 2009, **42**, 1584-1596.

30 J.-L. Bredas, J. E. Norton, J. Cornil and V. Coropceanu, *Acc. Chem. Res.*, 2009, **42**, 1691-1699.

31 C. D. Entwistle and T. B. Marder, *Angew. Chem. Int. Ed.*, 2002, **41**, 2927-2931.

32 S. Yamaguchi, T. Shirasake, S. Akiyama and K. Tamao, *J. Am. Chem. Soc.*, 2002, **124**, 8816-8817.

33 T. Agou, J. Kobayashi and T. Kawashima, *Org. Lett.*, 2006, **8**, 2241-2244.

34 T. Doda and Y. Shirota, *J. Am. Chem. Soc.*, 1998, **120**, 9714-9715.

35 W. L. Jia, X. D. Feng, D. R. Bai, Z. H. Lu, S. Wang and G. Vamvounis, *Chem. Mater.*, 2005, **17**, 164-170.

36 T. Node, H. Ogawa and Y. Shirota, *Adv. Mater.*, 1999, **11**, 283-285.

37 G. Zhou, C.-L. Ho, W.-Y. Wong, Q. Wang, D. Ma, L. Wang, Z. Lin, T. B. Marder and A. Beeby, *Adv. Funct. Mater.*, 2008, **18**, 499-511.

38 T. W. Hudnall, M. Melaimi and F. P. Gabbai, *Org. Lett.*, 2006, **8**, 2747-2749.

39 S. Yamaguchi, T. Shirasake and K. Tamao, *Org. Lett.*, 2000, **2**, 4129-4132.

40 Z. Zhou, S. Xiao, J. Xu, Z. Liu, M. Shi, F. Li, T. Yi and C. Huang, *Org. Lett.*, 2006, **18**, 3911-3914.

41 G.-L. Fu, H. Pan, Y.-H. Zhao and C.-H. Zhao, *Org. Biomol. Chem.*, 2011, *23*, 8141-8146.

42 M.-S. Lin, L.-C. Chi, H.-W. Chang, Y.-H. Huang, K.-C. Tien, C.-C. Chen, C.-H. Chang, C.-C. Wu, A. Chaskar, S.-H. Chou, H.-C. Ting, K.-T. Wong, Y.-H. Liu and Y. Chi, *J. Mater. Chem.*, 2012, **22**, 870-876.

43 P. Hohenberg and W. Kohn, *Phys. Rev. B*, 1964, **136**, 864-871.

44 W. Kohn and L. J. Sham, *Phys. Rev. A*, 1965, **140**, 1133-1138.

45 J. B. Foresman, M. H. Gordon, J. A. Pople and M. J. Frisch, *J. Phys. Chem.*, 1995, **96**, 135-149.

46 M. Cossi, N. Rega, G. Scalmani and V. Barone, *J. Chem. Phys.*, 2001, **114**, 5691-5701.

47 M. Cossi, G. Scalmani, N. Rega and V. Barone, *J. Chem. Phys.*, 2002, **117**, 43-54.

48 M. J. Frisch, G. W. Trucks, H. B. Schlegel, G. E. Scuseria, M. A. Robb, J. R. Cheeseman, J. A. Montgomery Jr., T. Vreven, K. N. Kudin, J. C. Burant, J. M. Millam, S. S. Iyengar, J. Tomasi, V. Barone, B. Mennucci, M. Cossi, G. Scalmani, N. Rega, G. A. Petersson, H. Nakatsuji, M. Hada, M. Ehara, K. Toyota, R. Fukuda, J. Hasegawa, M. Ishida, T. Nakajima, Y. Honda, O. Kitao, H. Nakai, M. Klene, X. Li, J. E. Knox, H. P. Hratchian, J. B. Cross, C. Adamo, J. Jaramillo, R. Gomperts, R. E. Stratmann, O. Yazyev, alvador, J. J. A. J. Austin, R. Cammi, C. Pomelli, J. W. Ochterski, P. Y. Ayala, K. Morokuma, G. A. Voth, P. S. Dannenberg, V. G. Zakrzewski, S. Dapprich, A. D. Daniels, M. C. Strain, O. Farkas, D. K. Malick, A. D. Rabuck, K. Raghavachari, J. B. Foresman, J. V. Ortiz, Q. Cui, A. G. Baboul, S. Clifford, J. Cioslowski, B. B. Stefanov, G. Liu, A. Liashenko, P. Piskorz, I. Komaromi, R. L. Martin, D. J. Fox, T. Keith, M. A. Al-Laham, C. Y. Peng, A. Nanayakkara, M. Challacombe, P. M. W. Gill, B. Johnson, W. Chen, M. W. Wong, C. Gonzalez and J. A. Pople, GAUSSIAN 03 (Revision B.05), Gaussian, Inc., Pittsburgh, PA, 2003.

49 M. Belletete, J. F. Morin, M. Leclerc and G. Durocher, *J. Phys. Chem. A*, 2005, **109**, 6953-6959.

50 J. Y. Jeon, T. J. Park, W. S. Jeon, J. J. Park, J. Jang, J. H. Kwon and J. Y. Lee, *Chem. Lett.*, 2007, **36**, 1156-1157.

51 Z. Ge, T. Hayakawa, S. Ando, M. Ueda, T. Akiike, H. Miyamoto, T. Kajita and M. Kakimoto, *Adv. Funct. Mater.*, 2008, **18**, 584-590.

52 J. N. Demas and G. A. Crobys, *J. Phys. Chem.*, 1971, **75**, 991-1024.

53 J. L. Brédas, R. Silbey, D. S. Boudreaux and R. R. Chance, *J. Am. Chem. Soc.*, 1983, **105**, 6555-6559.

54 J. Lee, J.-I. Lee, K.-I. Song, S.-J. Lee and H. Y. Chu, *Appl. Phys. Lett.*, 2008, **92**, 133304 (1-3).

55 J. Lee, N. Chopra, S. H. Eom, Y. Zheng, J. Xue, F. So and J. Shi, *Appl. Phys. Lett.*, 2008, **93**, 123306 (1-3).

56 V. Promaraka, and S. Ruchirawat, *Tetrahedron*, 2007, **63**, 1602-1609.

57 N. Li, S.-L. Lai, W. Liu, P. Wang, J. You, C.-S. Lee and Z. Liu, *J. Mater. Chem.*, 2011, **21**, 12977-12985.

58 J. H. Jou, M. F. Hsu, W. B. Wang, C. P. Liu, Z. C. Wong, J. J. Shyue and C. C. Chiang, *Org. Electron.*, 2008, **9**, 291-295.

Table 1. Physical properties of compound **BDDPC**

λ_{abs} (nm)	λ_{em} (nm)	Φ	HOMO (eV)		LUMO (eV)		E_g (eV)		T_d (^oC)	T_g (^oC)
348	420	0.95	Theo	Exp	Theo	Exp	Theo	Exp	234	110
390			-5.55	-5.61	-1.90	-2.35	3.65	3.26		

λ_{abs} : absorption peak maximum.
λ_{em} : emission peak maximum.
Φ : fluorescent quantum yield.
HOMO: highest occupied molecular orbital.
LUMO: lowest unoccupied molecular orbital.
E_g : energy gap between HOMO and LUMO.
T_d : decomposition temperature.
T_g: glass transition temperature

Table 2. Electroluminescent characteristics of Device R, G and B

Device	λ_{EL} (nm)	V_{on}	L_{max} (cd m^{-2})	$\eta_{L,max}$ (cd A^{-1})
R	624	3.0	12,337	11.04
G	508	2.5	26,473	38.60
B	472	3.0	7622	7.39

λ_{EL} : electroluminescence emission peak.
V_{on} : turn-on voltage at 1 cd m^{-2}.
L_{max} : maximum luminance.
$\eta_{L,max}$: maximum luminance efficiency.

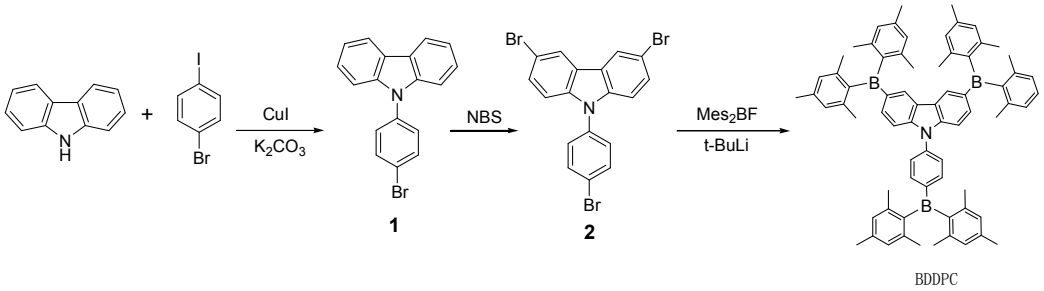

Scheme 1 The synthetic route of **BDDPC**.

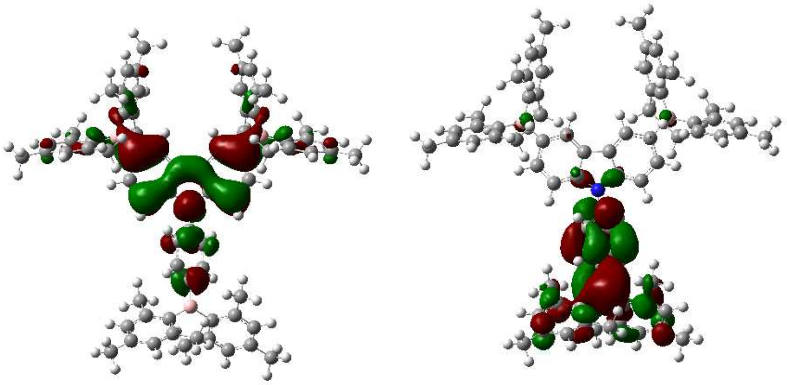

HOMO LUMO

Fig. 1. HOMO and LUMO diagrams of **BDDPC**.

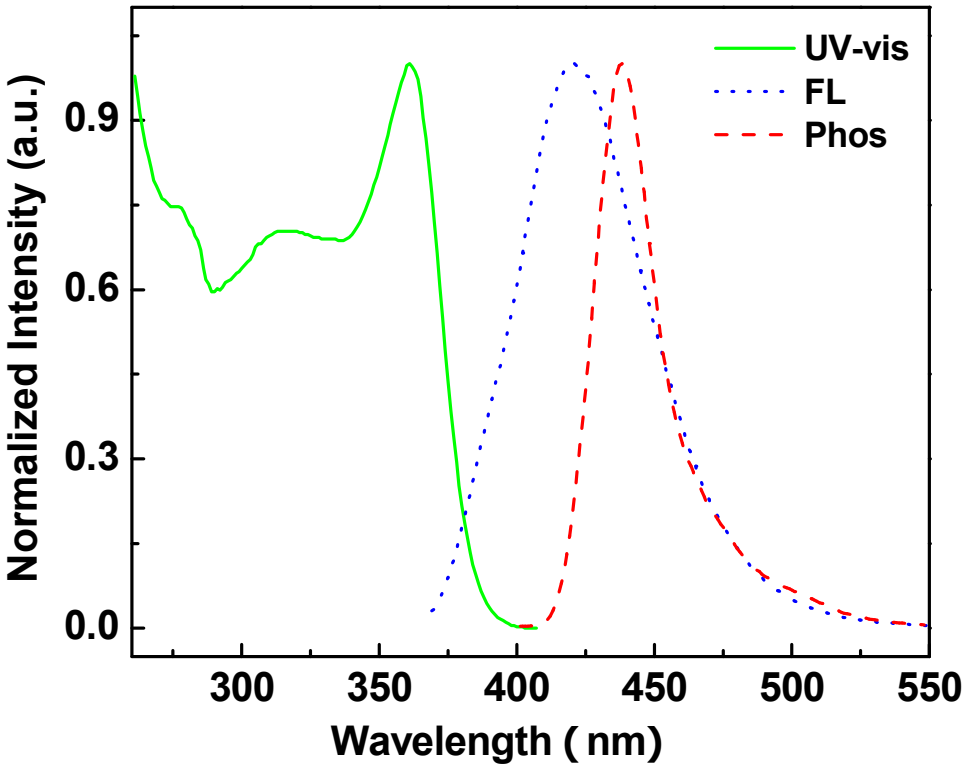

Fig. 2. UV-vis absorption, fluorescence (FL) and phosphorescence (Phos) spectra of **BDDPC**.

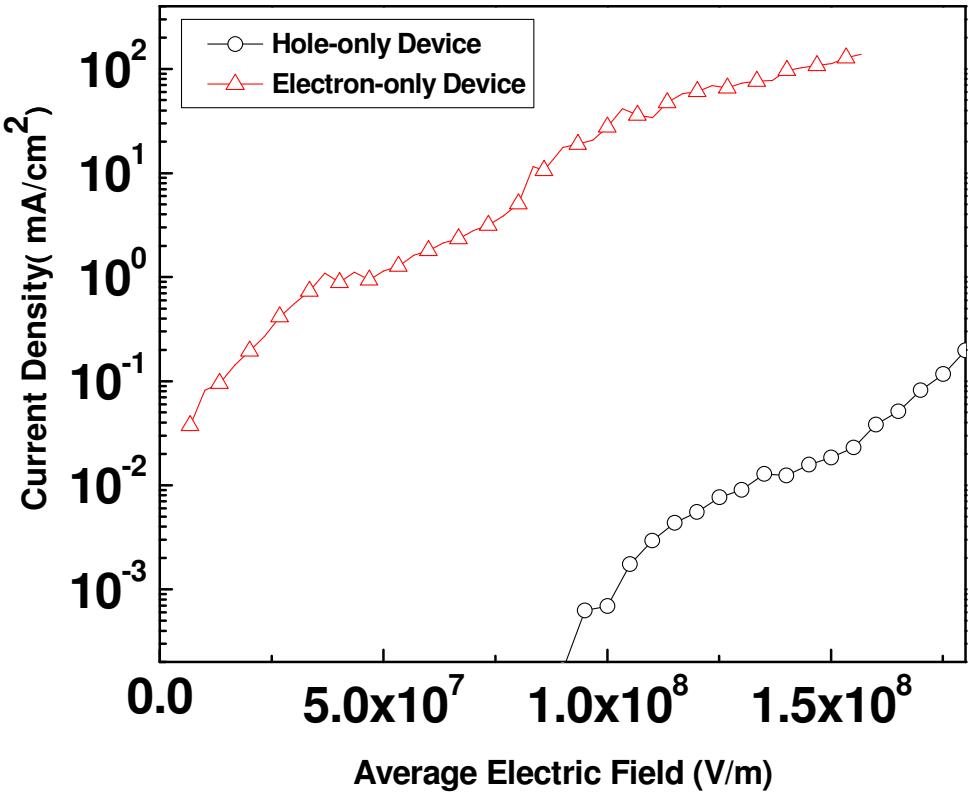

Fig. 3. The current characteristics as a function of the average electric field for hole-only and electron-only devices.

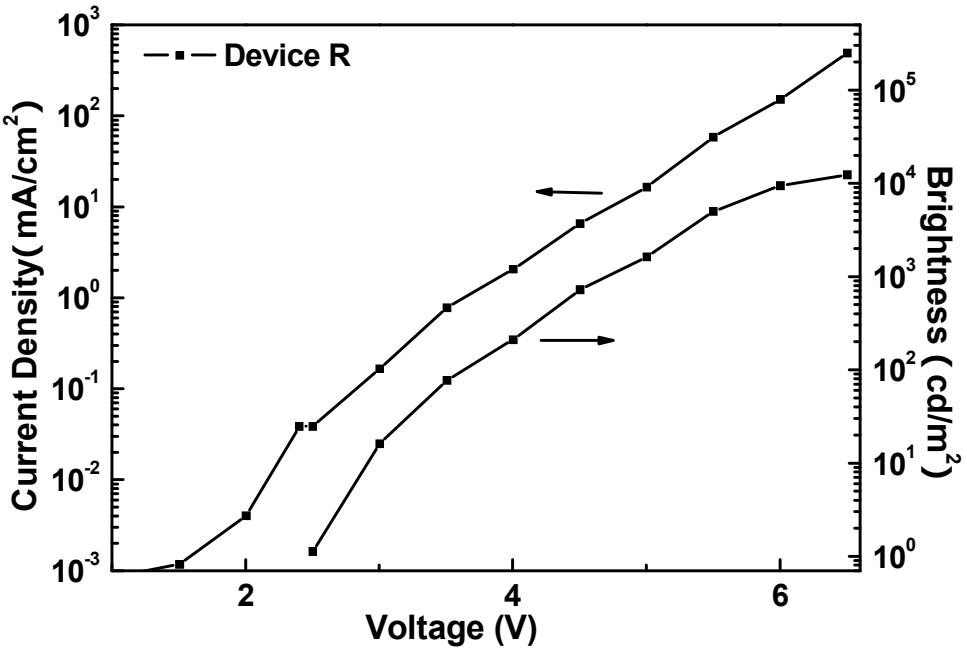

Fig. 4. Current density–voltage–luminance curves of Device R.

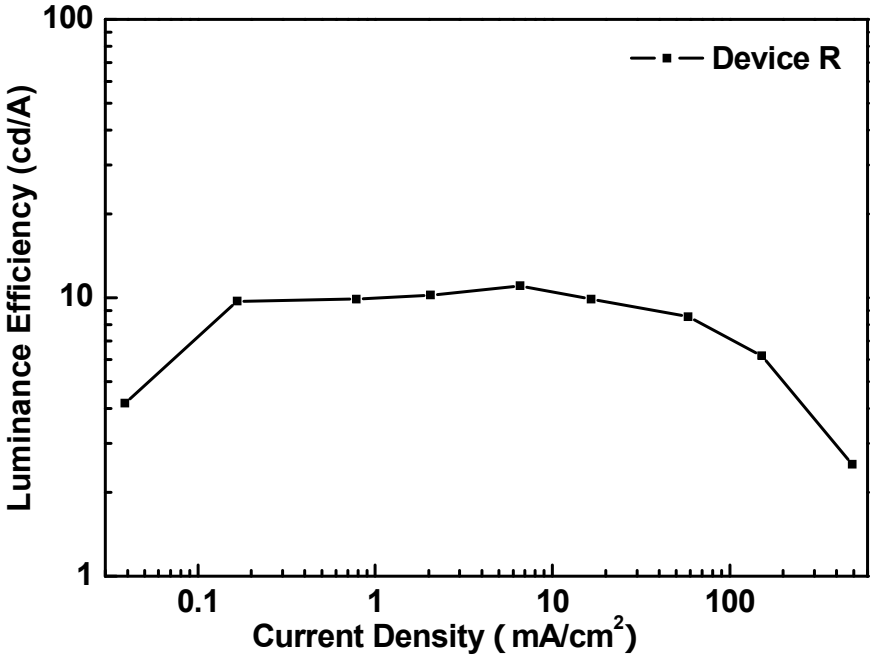

Fig. 5. Current density–luminance efficiency curve of Device R.

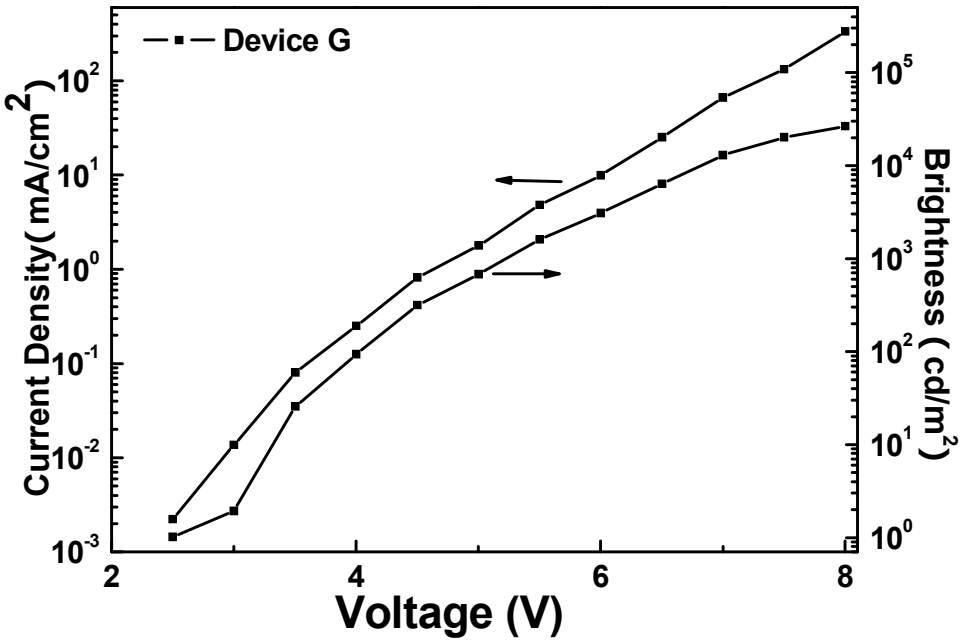

Fig. 6. Current density–voltage–luminance curves of **Device G**.

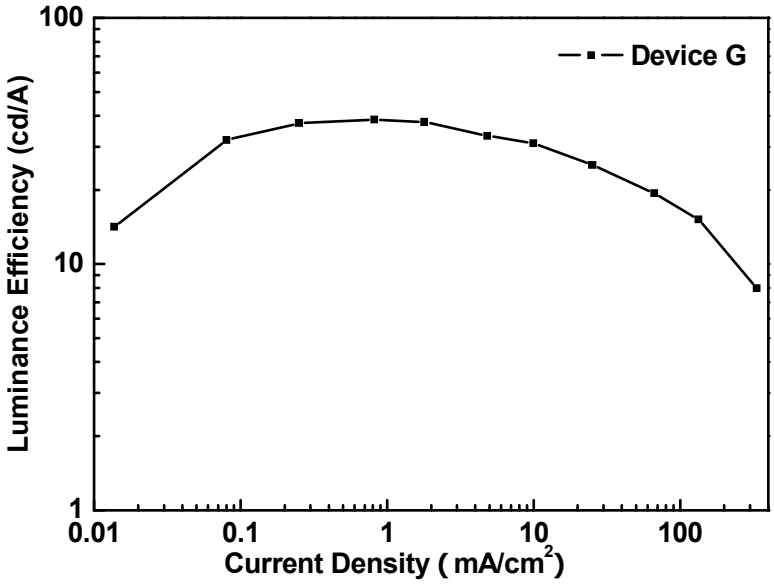

Fig. 7. Current density–luminance efficiency curve of **Device G**.

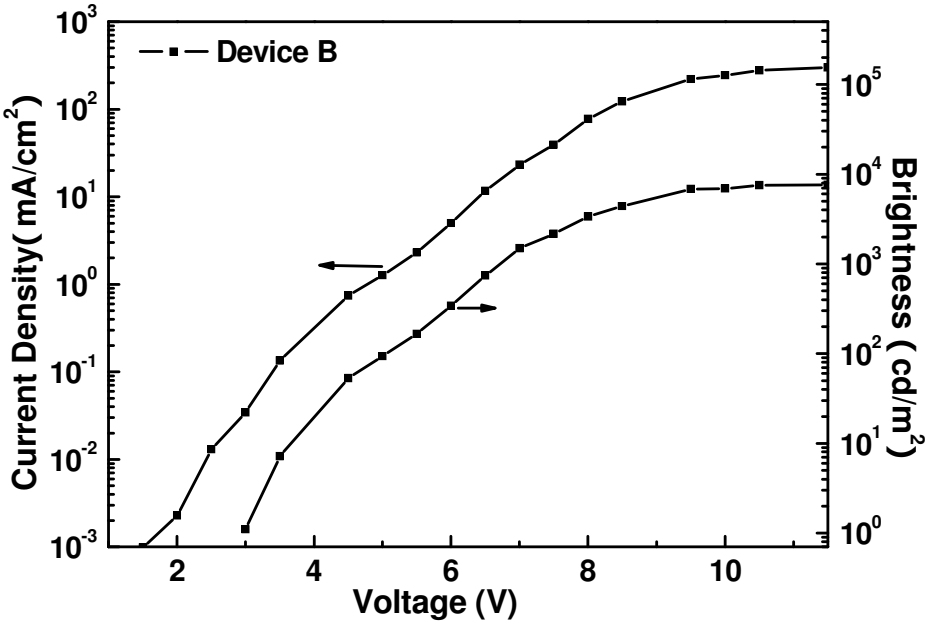

Fig. 8. Current density–voltage–luminance curves of **Device B**.

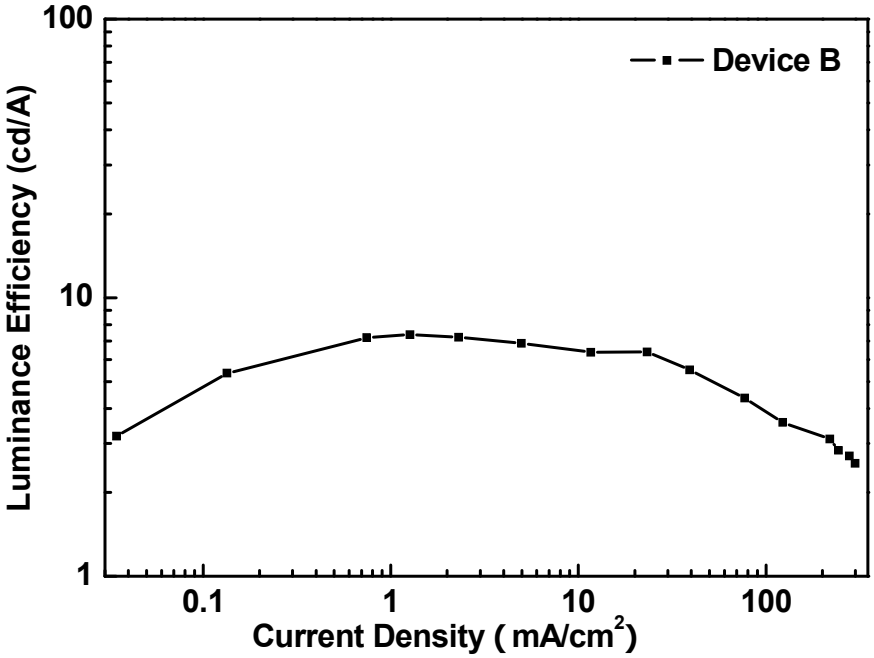

Fig. 9. Current density–luminance efficiency curve of **Device B**.